Effect of surface waves on the irradiance distribution in the upper ocean

Hemantha W. Wijesekera

College of Oceanic and Atmospheric Sciences, Oregon State University, 104 OC Admin Bldg, Corvallis, OR 97331
hemantha@coas.oregonstate.edu

W. Scott Pegau

Kachemak Bay Research Reserve, 95 Sterling Hwy, Suite 2, Homer, AK 99603
scott_pegau@fishgame.state.ak.us

Timothy J. Boyd

College of Oceanic and Atmospheric Sciences, Oregon State University, 104 OC Admin Bldg, Corvallis, OR 97331
tboyd@coas.oregonstate.edu

Abstract: The distribution of irradiance in the upper ocean was examined from sensors mounted on an Autonomous Underwater Vehicle (AUV). Apparent and inherent optical properties along with physical variability ranging from scales O(10 cm) to O(1 km) were collected off the coast of Oregon during the summer of 2004. Horizontal wavenumber spectra of downwelling irradiance showed that irradiance varied as a function of wavenumber and depth. The analysis indicates that irradiance variability between 1 and 20 m spatial scales was attributed to the focusing effects of surface wave geometry. The dominant wavelength of focusing at depths of 2 - 6 m was about 2 m for ~6 m s^{-1} wind speeds.

©2005 Optical Society of America

OCIS codes: (010.4450) Ocean optics; (120.5710) Refraction

References and links

1. Dera, J, *Marine Physics*, (Elsevier, Amsterdam, 1992, p.516).
2. Dera, J., S. S. Sagan, and D. Stramski, "Focusing of sunlight by sea surface waves: new results from the Black Sea,'' Oceanologia **34**, 13-25 (1993).
3. Melville, W. K., "The role of surface-wave breaking in air-sea interaction,'' Annu. Rev.Fluid Mech. **28**, 279-321 (1996).
4. Stramski, D., and J. Tegowski, "Effects of intermittent entrainment of air bubbles by breaking wind waves on ocean reflectance and underwater light field,'' J. Geophys. Res. **106**, 31,345-31,360 (2001).
5. Terrill, E. J., W. K. Melville, and D. Stramski, "Bubble entrainment by breaking waves and their influence on optical scattering in the upper ocean,'' J. Geophys. Res. **106**, 16815-16823 (2001).
6. Dera, J., and J. Olszewski, "Experimental study of short-period irradiance fluctuations under an undulating sea surface,'' Oceanologia **10**, 27 (1978).
7. Schneck, H., "On the focusing of sunlight by ocean waves, ''J. Opt. Soc. Am. **47**, 653-657 (1957).
8. Snyder R. L., and Dera J., "Wave-induced light field fluctuations in the sea,'' J. Opt. Soc. Am. **60**, 1072 (1970).
9. Zaneveld, J. R. V., E. Boss, and P. A. Hwang, "The influence of coherent waves on the remotely sensed reflectance, '' Opt. Express **9**, 260-261 (2001), http://www.opticsexpress.org/abstract.cfm?URI=OPEX-9-6-260.
10. Zaneveld, J. R. V., E. Boss, and A. Barnard, "Influence of surface waves on measured and modeled irradiance profiles,'' Appl. Opt. **40**, 1442-1449, (2001).

1. Introduction

The light field within the ocean varies as a result of several mechanisms. The variation of the solar zenith angle throughout the day creates a long period fluctuation. On shorter time scales

#8865 - $15.00 USD Received 22 September 2005; revised 30 October 2005; accepted 31 October 2005
(C) 2005 OSA

there are fluctuations associated with clouds and the surface wave field. Spatial variations may also result from the distribution of absorbing and scattering materials within the ocean. The focusing of light by the passage of waves is of particular interest here.

Surface waves ranging in wavelength from less than 1 cm to hundreds of meters to contribute to the geometry of the ocean surface. These waves have a major impact on light transmission at the air-sea sea interface and just below it. Steep-sloped capillary-waves focus light near the surface, and longer wavelength gravity waves focus light deeper in the water column. This wave focusing can cause the irradiance levels to increase several times the background level for short periods of time [1,2]. This focusing effect is related to wind speed through the wind-wave slope relationship. Interestingly, the focusing effect decreases at higher wind speed because the wave field becomes too complex to effectively focus light [1,2]. Below the surface, radiative transfer is dependent on the inherent optical properties (IOP) of the water column. A homogeneous distribution of absorbing materials will decrease the absolute intensity of fluctuations in irradiance caused by surface waves, but the relative intensity will remain the same. The scattering of light off particles and by water tends to diffuse the light field, resulting in decreased focusing of light. The path length of surface incident radiation increases with increasing depth, allowing scattering to reduce the fluctuations in the light field more at greater depth, and the most dynamic portion of the light field is thus in the upper 15 m of the water column.. Fluctuations in the underwater light field are largely a result of the incoming light field, slope of the sea surface, the IOP, and the depth of the measurement.

There are variations in the IOP at a broad range of scales, from the spacing between particles to meso-scale or larger variations created by major currents, and teasing apart the various contributions to the fluctuating light field can be difficult. For irradiance measurements, the effects of the variability at the smallest scales tend to average out because of the path-lengths of the various rays reaching subsurface detectors typically are much greater than the scale of variability. Processes that create variability in the IOP at scales of meters to kilometers can create variations in the light field. Breaking waves generate bubble clouds, which may penetrate well below the surface. Near-surface coherent structures such as Langmuir cells and shear-driven surface layer eddies can alter the distribution of bubble clouds, foam, particles and biological material, which can impact the irradiance distribution [3,4,5]. In contrast, the variability in irradiance due to the ocean-air interface is generally on smaller scales of centimeters to meters. These different processes are reflected in the irradiance power spectra.

Many studies of the variations in the light field have been conducted using fixed depth instrumentation [6,7,8]. To date, the interpretation of these studies has been limited by the lack of knowledge of the IOP associated with the water in which the study has been conducted. In the following we show the spatial variability of irradiance measurements along with physical and IOP measurements made from an Autonomous Underwater Vehicle (AUV).

2. Observations

Bio-optical property distributions over the continental shelf were examined using data collected during a research cruise off Oregon in the summer of 2004. During six days of sampling, we collected physical, optical, and biological data using several different platforms including an AUV, a lightweight towed platform, and a free-falling vertical profiler. The ocean data we discuss here was all collected with the AUV. The spatial structure of near-surface bio-optical and physical fields was obtained from sensors mounted on a Bluefin Odyssey III AUV. The 21” diameter, 11’ long AUV was equipped with an SBE25-CTD, an upward-looking 1200 kHz RDI ADCP and a downward-looking 300 kHz RDI DVL/ADCP, a microstructure package, a Satlantic ISUS nitrate sensor, a WETLabs AC9+ nine-channel optical spectrometer, an optical scattering sensor, and an upward looking 7-channel irradiance sensor.

#8865 - $15.00 USD Received 22 September 2005; revised 30 October 2005; accepted 31 October 2005
(C) 2005 OSA

Downwelling irradiance above the AUV was measured at 7 visible wavelengths with a Satlantic OCI-200. The sampling rate, the -3dB frequency, and the instrument time constant were 6 Hz, 3 Hz and 0.05 s, respectively. Coefficients of absorption and attenuation were measured with the WETLabs AC-9+ with a sampling rate of 6Hz and a path-length of 25 cm. The AC-9+ was mounted in the AUV and water was pulled from the nose cone by a pump mounted after the AC-9+. During processing the time lag for the 1.8 m of tubing was accounted for. Mixing within the tubing and the path-length of the instrument is likely to reduce the highest frequency variability. The AC-9+ was calibrated daily using deionized water. The turbulence package was mounted with the probes extending forward of the nose cone. Included in the package were fast-sampling (256 Hz) turbidity, pressure, and temperature sensors, two shear probes, and a 3-axis accelerometer. The 300 kHz DVL recorded the vehicle motion relative to the bottom for navigation. Meteorological measurements were made using an IMAT package mounted on the research vessel R/V New Horizon.

The AUV sampling was conducted as transects in an across-shelf/vertical plane, in which the upper part of the water column was sampled on either a saw-tooth trajectory or with repeated passes at different, fixed depths. Typical operating speeds of the AUV range from 3 to 4 knots. AUV sampling extended from the inner shelf (water depth ~ 50m) to the mid-shelf (water depth ~150m). At latitude 44.9ºN off Oregon this corresponds to distances of 4.34 to 18.47 km (2.37 to 10.07 nm) from the coast.

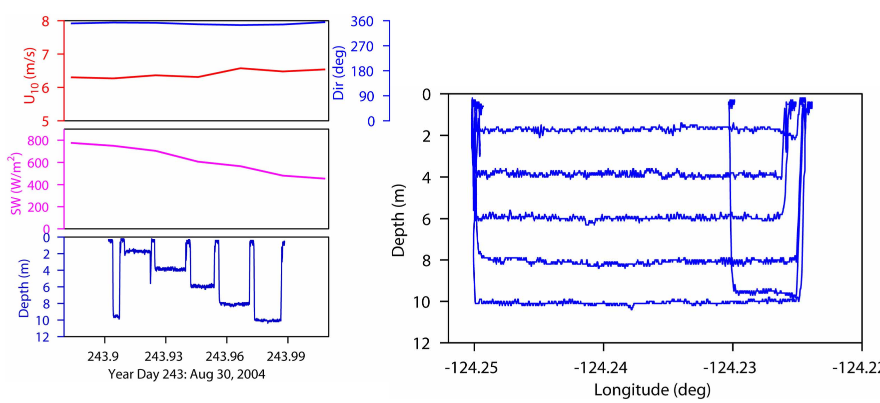

Fig. 1. An example of AUV level mission. The AUV level flights were conducted at 5 different depths during daytime hours while winds were blowing from north to south with a magnitude of about 6.5 m s^{-1} (wind stress ~ 0.054 N m^{-2}). Left Panels: wind speed and direction (top), short wave radiation (middle), and depths of AUV level flights as a function of time (bottom). Right Panel: Spatial position of AUV flights.

In the following, we describe a sub-set of the AUV data to demonstrate the effects of surface wave geometry on the irradiance distribution beneath a wave surface. An AUV mission consisting of a series of level transects (Fig. 1) was conducted, while the ocean was forced by steady southward winds of 6-7 m s^{-1} with intermittent breaking surface waves. The sky was clear of clouds and the shortwave radiation (400-1100 nm), as measured by the shipboard irradiance sensor, fell from about 700 W m^{-2} at the beginning to about 450 W m^{-2} at the end of the survey. The decline was monotonic and consistent with decreasing solar elevation on a clear day. The AUV conducted nearly 2-km long transects at 5 different pressure surfaces, measuring both physical and optical variability at horizontal scales ranging from O(cm) to O(km).

Received 22 September 2005; revised 30 October 2005; accepted 31 October 2005
(C) 2005 OSA

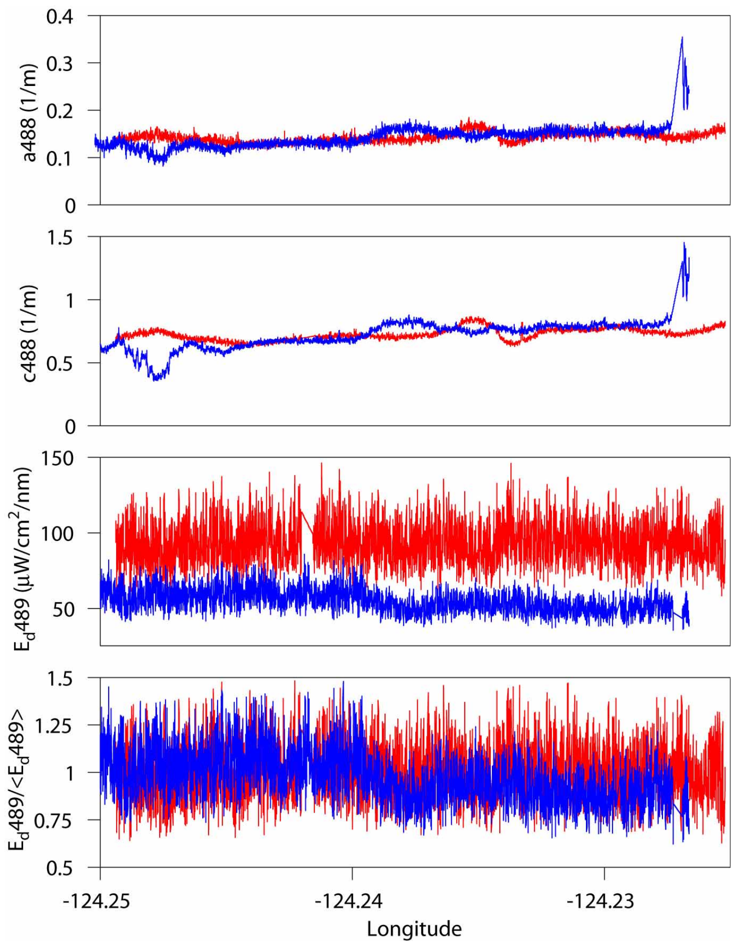

Fig. 2. From top to bottom: Spatial series of absorption and attenuation from AC-9+ , downwelling irradiance from OCI-200 for 2 m depth (red) and 4 m depth (blue), and normalized downwelling irradiance. Wavenumber spectra of IOP and irradiance for different depths are given in Figs. 3 and 4.

Time series of the absorption coefficient (a488) and attenuation coefficient (c488) at 488 nm, the downwelling irradiance at 489 nm (E_d489) at depths of 2 m and 4 m, and normalized E_d489 for those depths are shown in Fig. 2 as a function of location along the transect. All optical variables have been averaged in time to 0.2 s intervals, which is the equivalent of ~0.35 m intervals in space, prior to plotting. Fluctuations of E_d489 (referred to as Ed hereafter) were larger near the surface than at greater depths. The normalized Ed shows that the relative variability is nearly constant for the first half of the transect with lower relative variability observed at the 4 m level during the second half of the transect. There is also an increase in scattering relative to absorption at the same location. This result is consistent with our statement in the introduction that scattering will decrease the relative variability in the light field.

The wave-boundary layer has a positively skewed Ed distribution because the focusing of light rays beneath the wave-surface, where solar rays focus in a small regions compared to those where light divergence occurs. The skewness of Ed was estimated over AUV path-lengths from the measurements shown in Fig. 2, and was about 0.38 and 0.56 at 2 and 4 m, respectively. Dera *et al.* [2] reported that the wave induced focusing was strongest during

#8865 - $15.00 USD Received 22 September 2005; revised 30 October 2005; accepted 31 October 2005
(C) 2005 OSA

weak winds and was weakest during strong winds. They noted that the skewness of downwelling irradiance at a depth of 1 m below the surface in the Black Sea were about 1.53 and 0.59 for 2.7 m s^{-1} and 11.7 m s^{-1} wind speeds, respectively. The differences in our skewness estimates and that of Dera et al. [2] may be due to the difference in depth of the measurement.

3. Horizontal Wavenumber Spectra of Optical Fields

We have computed wavenumber spectra of IOPs and AOPs from the AUV level transect data. Power spectra of both c488 and turbidity are red in wavenumber space (Fig. 3), suggesting that the concentrations of biological and other particles are larger at lower wavenumbers, in particular at wavenumbers < 0.02 cycles per meter (cpm). We note that the Seapoint turbidity sensor, mounted at the front of the AUV and extending into to the free stream flow, has spatial resolution of about 10 cm, whereas the c488 spectra from the pumped AC9+ roll off at wavenumbers > 0.2 cpm, due to water exchange rates and path length to the sensor.

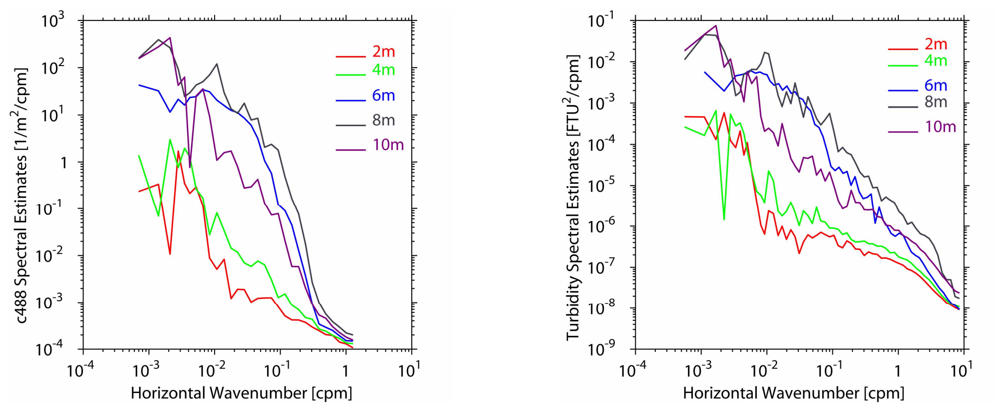

Fig. 3. Horizontal Wavenumber spectra of attenuation c488 (left) for different depths. Wavenumber spectra of turbidity (right) from the microstructure package. Turbidity which resolves spatial variability to about 10 cm, shows the red shape of IOP wavenumber spectra. Note: pumping rate of water limited the spatial resolution of AC9 signals to about 2 m (or 0.5 cpm). Most of the IOP variability is at scales greater than 100 m.

The wavenumber spectrum of irradiance fluctuations varies as a function of depth (Fig. 4). The spectrum at 2 m is approximately nearly constant in amplitude, whereas the spectrum 10 m has the smallest amplitudes at higher wavenumbers. Although spectral properties are different at higher wavenumbers, both shallow and deep water spectra have similar magnitudes at the low wavenumber end (< 0.005 cpm). It is possible that AUV motion can modify Ed measurement. The AUV has a distinct control cycle: fluctuations in pitch and depth show ~ 10 s period while fluctuations in roll show a ~ 5 s period. We examined coherences between Ed and pitch, roll, and depth of the AUV (Fig. 5), and found that the vehicle motion had a negligible impact on Ed. Similar coherences between Ed and c488 and a488 were computed (not shown here) and found that IOP has a negligible impact on Ed variability at higher wavenumbers. The conclusion can be drawn from Fig. 4 is that the changes in spectral shapes as a function of depth is simply due to the focusing of solar rays by surface wave geometry.

#8865 - $15.00 USD Received 22 September 2005; revised 30 October 2005; accepted 31 October 2005
(C) 2005 OSA

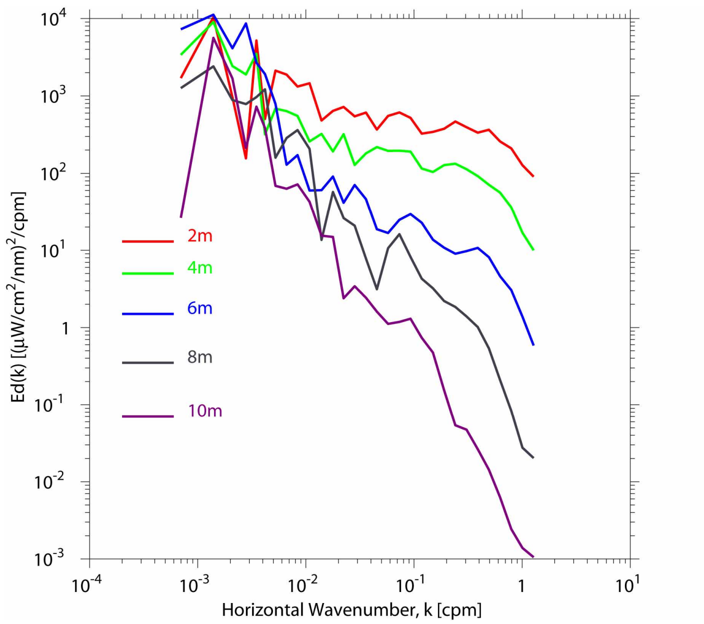

Fig. 4. Horizontal wavenumber spectra of downwelling irradiance Ed at 489nm wavelength. Wave focusing of light appears to be responsible for the spatial energy at large wavenumbers (for example see Zaneveld *et al.*, [9,10]).

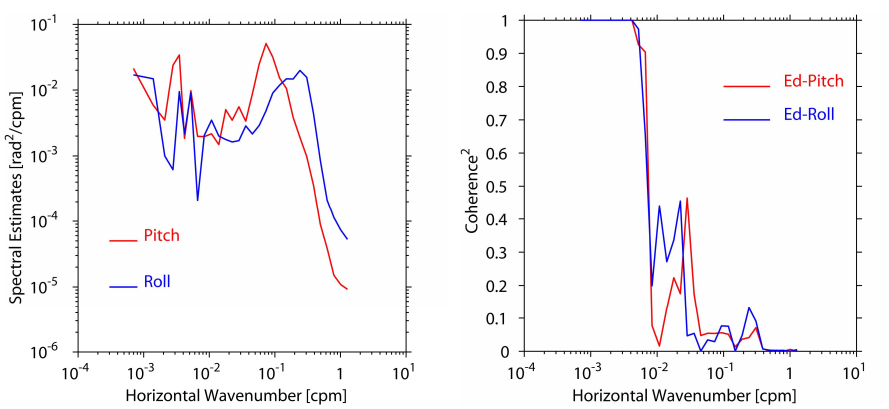

Fig. 5. Left Panel: Horizontal wavenumber spectra of pitch (red) and roll (blue) at a depth of 2 m. Right Panel: Coherence between Ed at 2 m (Fig. 4) and vehicle's pitch and roll at 2 m; Ed-pitch coherence (red) and Ed-roll coherence (blue). Coherences between Ed and the vehicle's pitch and roll in the 0.05 - 1 cpm wavenumber band are quite small and do not contribute the to irradiance measurement.

The normalized energy preserving spectrum for a given depth, $kEd(k)/\langle Ed\rangle^2$ was computed by first multiplying the Ed(k) spectrum by wavenumber, k, and then dividing by $\langle Ed\rangle^2$ at that depth, where angle brackets denote the mean. <Ed> decreased exponentially with depth, and the mean values of irradiance at 2, 4, 6, 8, and 10m are 93.5, 56.6, 29.8, 17.7, and 6.8 μW cm^{-2} nm^{-1}, respectively. The energy preserving spectrum has a local peak before

#8865 - $15.00 USD Received 22 September 2005; revised 30 October 2005; accepted 31 October 2005
(C) 2005 OSA

it rolls off at high wavenumber end (Fig. 6). For example, the spectrum at 2 m peaks near 0.4 - 0.6 cpm. i.e., the focusing of solar rays dominated at ~ 2 m horizontal scales.

The depth at which light is focused, z_f, depends only on the wave steepness, $\delta = A/L$, and can be approximated as

$$z_f / L = 2\delta + 1/(8\delta), \tag{1}$$

where A is the amplitude and L is the wavelength [10]. The wave steepness δ is large for the gravity-capillary wave band, and those waves focus light at a short distance from the wave surface. Longer gravity waves with small δ can focus light to greater depths. Scattering events are concentrated at the intersection points of focusing light rays, thus capillary waves contribute to a diffuse irradiance field just beneath the surface by capillary waves.

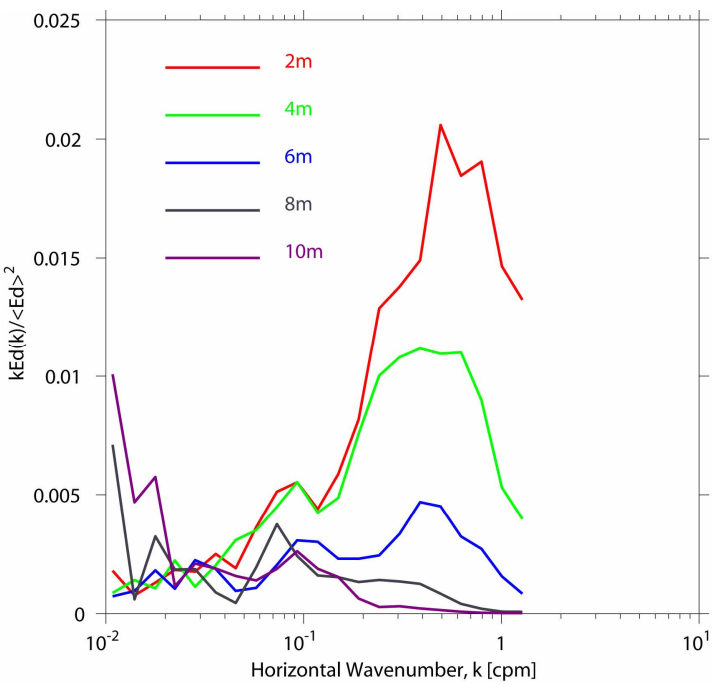

Fig. 6. Normalized area preserving spectra of irradiance for 5 different depths shown in Fig. 4. Spectral estimates for wavenumbers greater than 0.01 cpm are plotted.

Zaneveld *et al.* [9,10] reported that the vertical extent of the irradiance pattern beneath a sinusoidal wave surface is a function of δ. They showed that the irradiance pattern beneath a sinusoidal wave scales horizontally by wavelength, L, and vertically by,

$$z_c / L = 0.5 \tan\left[\pi/2 + a\sin\left\{n^{-1}\sin\left(a\tan(2\pi\delta)\right)\right\} - a\tan(2\pi\delta)\right], \tag{2}$$

where a is the absorption coefficient, and n is the refractive index of the water [10]. This scaling results in a diamond shaped irradiance pattern in a horizontal/vertical plane (see Fig. 4 in Zaneveld *et al.*, [10]). As demonstrated by Zaneveld *et al.* [10], the superposition of O(cm) capillary waves can make a drastic change in the underwater irradiance pattern, especially generating smaller-scale focusing patterns beneath the surface with reduced intensity of focused light at the highest amplitude wave-band at greater depths. By taking account of findings from theoretical and numerical modeling studies [9,10], we argue that the wavelength corresponding to the peak of the spectrum shown in Fig. 6 may represent the

#8865 - $15.00 USD Received 22 September 2005; revised 30 October 2005; accepted 31 October 2005
(C) 2005 OSA

dominant gravity wave scale during our observations. The spectral roll-off at the highest wavenumbers indicates that the effect of focusing by capillary and gravity-capillary waves may be limited to just beneath surface, while providing a diffusive light below 2 m. We expect a shift in spectral peak toward higher wavenumbers at shallower depths (say, depths less than 1 m), where focusing of light rays is dominated by small-scale gravity-capillary waves.

4. Conclusions

We conducted nearly a week long AUV bio-optical survey over the Oregon continental shelf on August 2004. Horizontal wavenumber spectra of downwelling irradiance show that irradiance varies as a function of wavenumber and depth. It is likely that irradiance variability between 1 and 20 m horizontal spatial scales was due to the focusing effects of surface wave field, since the IOP variability contributes little in that wavenumber band. This indicates that IOP most likely did not affect the results of previous studies of high-frequency variability in the light field. The dominant wavelength of focusing at depths of 2 - 6 m was about 2 m.

Acknowledgments

This research was supported by grants from Office of Naval Research, N00014-02-1-0104, N0014-03-0484 and N0014-03-0407. We are grateful to the master and crew of the R/V New Horizon for their contributions to a successful cruise and to C. Waluk, G. May, and I. Maccallum for cruise preparations, assisting the operation of AUV, and processing of AUV data sets. For assistance aboard the R/V New Horizon, we are indebted to A. Erofeev, A. Dale, S. Pierce, C. Wingard, R. O'Malley, and T. Cowels. Discussion and comments given by Clayton Paulson and Ronald Zaneveld are greatly appreciated.